Title

Undermining Glutaminolysis Bolsters Chemotherapy While NRF2 Promotes Chemoresistance in KRAS-Driven Pancreatic Cancers

Journal

Cancer Research, 80(8)

ISSN

0008-5472

Authors

Mukhopadhyay, Suman
Goswami, Debanjan
Adiseshaiah, Pavan P
et al.

Publication Date

2020-04-15

DOI

10.1158/0008-5472.can-19-1363

Peer reviewed

HHS Public Access

Author manuscript

Cancer Res. Author manuscript; available in PMC 2020 April 27.

Published in final edited form as:

Cancer Res. 2020 April 15; 80(8): 1630–1643. doi:10.1158/0008-5472.CAN-19-1363.

Undermining glutaminolysis bolsters chemotherapy while NRF2 promotes chemoresistance in KRAS-driven pancreatic cancers

Suman Mukhopadhyay[1,2], **Debanjan Goswami**[1,2], **Pavan P. Adiseshaiah**[2], **William Burgan**[1,2], **Ming Yi**[1,2], **Theresa M. Guerin**[3], **Serguei V. Kozlov**[3], **Dwight V. Nissley**[1,2], **Frank McCormick**[1,2,4]

[1]National Cancer Institute- RAS Initiative, Frederick National Laboratory for Cancer Research

[2]Cancer Research Technology Program, Frederick National Laboratory for Cancer Research, Frederick, Maryland 21701, USA

[3]Center for Advanced Preclinical Research, Frederick National Laboratory for Cancer Research, National Cancer Institute, Frederick, Maryland 21702, USA

[4]Helen Diller Family Comprehensive Cancer Center, University of California, San Francisco, California 94158, USA

Abstract

Pancreatic cancer is a disease with limited therapeutic options. Resistance to chemotherapies poses a significant clinical challenge for pancreatic cancer patients and contributes to a high rate of recurrence. Here we showed that oncogenic KRAS, a critical driver of pancreatic cancer, promotes metabolic reprogramming and upregulates NRF2, a master regulator of the antioxidant network. NRF2 contributed to chemoresistance and was associated with a poor prognosis in pancreatic cancer patients. NRF2 activation metabolically rewired and elevated pathways involved in glutamine metabolism. This curbed chemoresistance in KRAS-mutant pancreatic cancers. Additionally, manipulating glutamine metabolism restrained the assembly of stress granules, an indicator of chemoresistance. Glutaminase inhibitors sensitized chemoresistant pancreatic cancer cells to gemcitabine, thereby improving the effectiveness of chemotherapy. This therapeutic approach holds promise as a novel therapy for pancreatic cancer patients harboring KRAS mutation.

Graphical Abstract

Corresponding Author: Frank McCormick, Helen Diller Family Comprehensive Cancer Center, University of California, San Francisco, 1450 3rd Street, San Francisco, CA 94158 Phone: (415) 502-1707; Fax: (415) 502-1712; frank.mccormick@ucsf.edu.

Disclosure of Potential Conflicts of Interest

Dr. Frank McCormick is a consultant for the following companies: Aduro Biotech, Amgen, Daiichi Ltd, Ideaya Biosciences, Kura Oncology, Leidos Biomedical Research, Inc., PellePharm, Pfizer Inc., PMV Pharma, Portola Pharmaceuticals, and Quanta Therapeutics. Dr. McCormick has received research grants from Daiichi Sankyo Ltd and is a recipient of funded research from Gilead Sciences. Dr. McCormick is a consultant and co-founder for the following companies (with ownership interest including stock options): BridgeBio, DNAtrix Inc., Olema Pharmaceuticals, Inc., and Quartz. Dr. McCormick is Scientific Director of the NCI Ras Initiative at Frederick National Laboratory for Cancer Research/Leidos Biomedical Research, Inc.

Oncogenic KRAS-induced NRF2 upregulates glutaminolysis. Targeting glutamine metabolism downregulates chemoresistance markers, diminishes stress granule accumulation and dampens GPX4. Restricting glutaminolysis bolsters the effect of gemcitabine against pancreatic cancer.

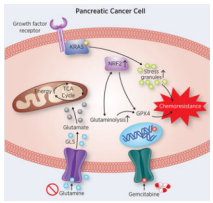

Keywords

Pancreatic cancer; chemotherapy; drug resistance; KRAS; NRF2; Glutamine metabolism; gemcitabine; CB-839

INTRODUCTION

Pancreatic cancer ranks among the deadliest and most aggressive malignancies (1). Late-stage diagnoses limit surgical intervention, so radiation and chemotherapy become standards of care. However, given its resistance to established therapeutic regimens, including gemcitabine, a frontline chemotherapeutic agent for pancreatic cancer (2,3), novel therapeutic approaches for pancreatic cancer patients are desperately needed. Most pancreatic ductal adenocarcinomas (PDACs) harbor mutationally activated KRAS, most often at position G12D (4). Unfortunately, KRAS G12D itself is not yet druggable (5). Thus, alternative strategies are needed.

Oncogene-directed metabolic reprogramming is an emerging hallmark in cancer (6,7). KRAS promotes metabolic rewiring, presenting opportunities for novel therapeutic strategies (4,8,9). To meet its increased anabolic need and support proliferation and survival, mutant KRAS upregulates glycolysis and alters glutamine metabolism (1,4,10,11) by increasing glutamine uptake (12) and reprogramming glutaminolysis (1,13).

Mutant KRAS confers chemoresistance by activating the transcription factor NRF2, encoded by *NFE2L2*, a critical contributor to the cellular stress response (14–16). Aberrant activation of NRF2 promotes pancreatic tumorigenesis. NRF2 regulates the expression of a battery of cytoprotective genes, including those involved in drug detoxification and redox balance (17,18), and it plays a critical role in anabolic cancer metabolism by altering glucose and glutamine metabolism (19). Though activated NRF2 has recently been linked to upregulated glutamine dependency in cancer cells (20), the impact of NRF2 in KRAS-driven PDAC cell metabolic rewiring is less well characterized.

We investigated the role of NRF2 in PDAC by first analyzing NRF2 expression levels in pancreatic tissues and cell lines. We observed variable expression of NRF2 and identified elevated NRF2 levels in higher-grade pancreatic cancer tissues. We also show that PDACs with significantly elevated NRF2 expression are more chemo-resistant. We provide evidence that elevated levels of NRF2 in PDACs are responsible for metabolic alterations—

specifically, pathways that are regulated by glutamine metabolism. We perturbed glutamine metabolic pathways and showed that inhibiting glutaminolysis in PDACs can overcome gemcitabine resistance. Significantly, targeting glutamine metabolism via glutaminase inhibitors may be an effective strategy for treating PDACs harboring KRAS mutations.

MATERIALS AND METHODS

Cell Culture and Reagents

All cell lines used in this study were obtained from the RAS Reagent Core (Frederick National Laboratory for Cancer Research, Frederick, MD). Cell line identities were confirmed by short tandem repeat analysis. Cell lines were tested for mycoplasma, authenticated before and at several points throughout the study, and maintained under conditions described by the vendor. See supplementary methods for details.

For stable cell line generation, control cell lines were generated using Precision LentiORF RFP Positive Control (#OHS5833, Dharmacon), and NRF2 overexpressing lines were generated using Precision LentiORF NFE2L2 w/o Stop Codon (#OHS5900–202624558, Dharmacon, Lafayette, CO) lentiviruses. Cells were expanded in selection media for a minimum of one week prior to further experimentation.

Non-essential amino acid (NEAA) solution (#11140) was purchased from Gibco. Erastin (5449) was obtained from Tocris Bioscience. AI-1(SML0009), DMKG/ Dimethyl 2-oxogluterate (#349631), 5-Fluorouracil (5-FU #F6627), and Capecitabine (SML0653) were purchased from Sigma-Aldrich. BPTES (S7753) and RSL3 (S8155) were obtained from Selleckchem. Gemcitabine (#3259) was obtained from Tocris Bioscience. CB-839 (#B0084–462472) was purchased from BOC Sciences.

Transient Transfection

Cells were plated at 70% confluence in medium containing 10% serum. Standard protocol was followed (21). In short, after 24 h of plating, cells were transfected with shRNA or overexpressing plasmids using Lipofectamine 3000 (Invitrogen) according to the manufacturer’s instructions. NFE2L2 mission shRNA plasmids (TRCN00007555, TRCN00007558) and mission control shRNA plasmid (SHC002) were obtained from Sigma. For transient overexpression, NFE2L2 overexpressing plasmid was purchased from DNASU (# HsCD00079566), and control plasmid with a similar backbone (#V37006) was purchased from Invitrogen.

Western Blot Analysis

A standard immunoblotting method was followed (21). Briefly, cell lysates were collected using M-PER (Thermo Fisher Scientific, 78501) and proteins were separated on denaturing SDS-PAGE gels (Bio-Rad). Electrophoresed proteins were transferred to nitrocellulose membranes. After transfer, membranes were blocked in an isotonic solution containing 5% non-fat dry milk in TBS. Membranes were incubated with primary antibodies as described in the text, and depending on the origin of the primary antibody, either anti-mouse or anti-rabbit HRP (Pierce) conjugated IgG was used for detection using the ECL system (Pierce).

Immunofluorescence and Immunohistochemistry

For immunofluorescence experiments, cells were permeabilized, incubated with indicated antibodies, and visualized by inverted microscope. For immunohistochemistry, slides were stained on the Discovery Ultra System (Roche) following the manufacturer's instruction and scanned on the Digital Pathology Scanner (Leica). Further details are in the supplementary methods.

Cell Proliferation and Viability Assays

Cell proliferation assays were conducted under different drug or media conditions. At the indicated times, cells were washed with PBS, trypsinized, stained with crystal violet, and counted. Cell viability was assessed using the CellTiter-Glo assay (#G-8461, Promega) following Promega's instructions. IC50 was calculated using GraphPad Prism.

Metabolomic and Lipidomic Analysis

Cells were trypsinized followed by washing and resuspension with D-PBS (#14190–144, Gibco). Samples were frozen and transferred to NIH-WCMC (metabolomics) and Lipotype (lipidomics) for detailed analysis.

Bioinformatics Analysis

The pancreas cancer data sets from Oncomine (https://www.oncomine.org/resource/) were used for various metabolic gene analyses. Parameters for each Oncomine data analysis are mentioned in the figures.

TCGA-PAAD survival curves for NFE2L2 and NFE2L2/KRAS expression were assessed using the PROGgeneV2 webtool (http://watson.compbio.iupui.edu/chirayu/proggene/database/index.php). The data were presented with p values with limits at the 75^{th} and 25^{th} percentiles. The parameters used in the analysis are mentioned in the figures.

Metabolic genes up-regulated in PAAD at later stage (stage II) or higher grade (grade 3) compared to Stage I or grade 1, respectively, in RNAseq data of TCGA PAAD patients. t-test analysis was used to determine p values. Oncomine analysis was also used to determine the up-regulated metabolic genes in higher-grade PAAD tissues in copy number of TCGA PAAD patients. Threshold p-values used in the analysis are mentioned in the figure.

For The Cancer Genome Atlas data (TCGA) clinical attributes and GSEA analysis, we analyzed data on significance of pathways/terms from GOBP, and pathway databases using the GSEA method, which closely followed the previously described method (22).

Xenograft Studies

Animal work was performed in accordance with the guidelines for animal welfare and protocols approved by the IACUC. Twenty (n=5 mice/group) nude mice (Jackson Laboratory) had 5×10^6 PANC-1 or SU.86.86 or MIA PaCa-2 cells implanted on the left flank. Cells were resuspended in PBS then mixed with an equal volume of Matrigel (Corning 354234) before sub-cutaneous implantation into mice. The animals were randomized when tumors reached a mean volume of $100mm^3$ and assigned to the indicated

groups. Treatment was continued until Day 38 (PANC-1, MIA PaCa-2) or Day 34 (SU.86.86).

KPC Allografts

Murine pancreatic adenocarcinoma cell line KPC (Pdx1-Cre$^{tg/+}$; Kras$^{G12D/+}$; Tp53$^{R172H/+}$) developed from spontaneous primary PDAC tumors in triple transgenic mice bearing a combination of genetically engineered Pdx-1-Cre$^{tg/+}$, Kras$^{SLS\text{-}G12D/+}$, and p53 R172H$^{LSL\text{-}R172H/+}$ alleles was provided by the NCI's Center for Advanced Preclinical Research. C57bl/6J mice (Jackson Laboratory) received a subcutaneous inoculum of KPC cells. Upon engraftment, animals were allowed to develop palpable lesions (<4 mm^3 tumor volume) and then randomized into treatment groups and treated with drugs as indicated.

Statistics

Data are expressed as mean ± SEM of at least three independent experiments. Statistical analysis was done using Excel or GraphPad 8. Probability <0.05 was considered the statistical significance threshold.

RESULTS

NRF2 Expression in Pancreatic Cancers

NRF2 is induced by oncogenic KRAS and is critical for tumor progression (14,15,23). To investigate the connection between KRAS and NRF2 in PDAC, we used a pair of human pancreatic ductal epithelial stable cell lines (HPNE cells; human pancreatic nestin expressing cells, ATCC CRL 4023), one expressing wild-type (WT) KRAS and the other a mutant KRAS G12D. As expected, we observed dramatic activation of NRF2 and known downstream effectors (17) of the NRF2 pathway (NQO1, GCLC, AKR1C1, and HMOX1) in the KRAS G12D HPNE compared to KRAS WT HPNE (Fig. 1A, Supplementary Fig. S1A). Oncomine analysis indicated a 2.2-fold induction of NRF2 expression in KRAS mutant pancreatic cancer compared to KRAS WTs (Supplementary Fig. S1B). Further analysis through cBioPortal on PDAC samples revealed that 21% have elevated NRF2 mRNA expression and concurrent upregulation in KRAS expression (Supplementary Fig. S1C). Using TCGA-PAAD data, we evaluated the effect of combined NRF2-KRAS expression on patient survival. Patients with lower expression of the NRF2-KRAS gene set combination (Supplementary Fig. S1D, E) had longer survival. TCGA-PAAD data also demonstrate upregulation of NRF2 in mutant KRAS compared to WT (Supplementary Fig. S1F). Next, we chose a panel of six PDAC cell lines to check NRF2 basal levels. Surprisingly, we found differential expression of NRF2 in those lines (Fig. 1 B, C). We also found, at least within this panel, that KRAS G12D mutant cells (Supplementary Fig. S1G) have substantial NRF2 protein levels, which is significant, as G12D is the prevalent mutation in pancreatic cancer (4). We further examined the basal level of NRF2 in another tumor model (Kras$^{G12D/+}$; Tp53$^{R172H/+}$) KPC mouse pancreas tissue. NRF2 protein levels are also upregulated in KPC mouse PDAC tissues compared to normal pancreatic tissue (Fig. 1D). Taken together, these data reflect a variation of intensity in NRF2 expression among PDAC samples.

To further characterize levels of NRF2 expression in PDAC, we analyzed human pancreatic cancer tissue microarrays, including PDAC tissue samples and normal pancreas tissue (Fig. 1E, Supplementary Fig. S2A) with patient clinicopathological features (Supplementary Table S1). The accumulated intensity of IHC staining of NRF2 revealed a wide range in all tissue groups. Further analysis demonstrated diverse staining scores according to accumulated intensity and revealed that the majority (63% of grade 3 and 58% of grade 2) of higher-grade PDAC tissue samples showed intermediate and strong NRF2 staining compared to grade 1 samples (33% of mild staining). These data (Fig. 1F) illustrate the presence of NRF2 in poorly differentiated high-grade PDAC tissue samples (strong staining in grade 3: 26%), which are more aggressive. Among well-differentiated low-grade samples, we did not see strong staining of NRF2. Concurrently, 67% of grade 1 tissue samples in our study had weak staining scores. Surprisingly, certain normal pancreas tissues had moderately high levels of NRF2 based on staining intensity. This could be caused by several factors. Multiple studies have reasoned that NRF2 upregulation protects cells from stress stimuli including environmental agents/drugs, inflammatory stresses, and chronic exposure to carcinogens such as cigarette smoke. Moreover, NRF2 signaling is induced by medications for diabetes, pancreatitis, and other diseases (24,25), which could have influenced NRF2 expression in some normal tissues. However, after thorough analysis of the human tissue microarray, our data indicate a possible correlation between NRF2 expression and higher-grade PDAC tissue samples. Elevated NRF2 expression associated with tumor progression is also seen in TCGA-PAAD survival data. Kaplan-Meier analysis shows a significant difference in outcome when patients are separated by high and low NRF2 expression levels (Fig. 1G, Supplementary Fig. S2B). Therefore, NRF2 expression is associated with a poor clinical outcome. Oncomine analysis also validates elevated levels of NRF2 in PDAC compared to a normal pancreas (Fig. 1H). Taken together, our data demonstrate that NRF2 is expressed over a wide range that, in turn, correlates with the clinical status of KRAS-driven pancreatic cancer.

Modulating NRF2 expression regulates sensitivity of PDAC cells to gemcitabine

Oncogenic KRAS enhances chemoresistance by upregulating NRF2 signaling (15). Gemcitabine, which interferes with DNA synthesis, is used for treating PDAC patients, though its efficacy is limited (2). It's been shown that long-term gemcitabine treatment leads to NRF2 activation, resulting in chemoresistance (26). Therefore, we examined whether differential expression of NRF2 in PDAC cells is linked to gemcitabine sensitivity. We measured the sensitivity of PDAC cells to gemcitabine and observed that cells with higher levels of NRF2 had higher IC_{50} values (Fig. 2A, Supplementary Table S2A). Knocking down NRF2 using two different sequences of shRNAs (Supplementary Fig. S3A) elicited a significant increase in gemcitabine sensitivity (Fig. 2B, Supplementary Table S2B). We then used AI-1, a well-characterized, potent pharmacological activator of NRF2 that covalently modifies Keap1 to activate NRF2 (27), in PANC-1 cells (Supplementary Fig. S3B). Remarkably, it increased NRF2 expression in PANC-1 cells (higher NRF2 basal levels) and increased gemcitabine resistance (Fig. 2C, Supplementary Table S2C). Overexpressing NRF2 in PDAC cells (Supplementary Fig. S3C), which have a low basal level of NRF2, increased gemcitabine resistance (Fig. 2D, Supplementary Table S2D). Taken together, our data indicate that NRF2 levels regulate the sensitivity of PDAC cells to gemcitabine. We

then used AI-1 to activate NRF2 in BxPC-3 and MIA PaCa-2 cells (Supplementary Fig. S3D) and tested gemcitabine sensitivity. Cells became significantly more resistant to gemcitabine upon AI-1 treatment (Fig. 2E, Supplementary Table S2E). We also observed that knocking down NRF2 (Supplementary Fig. S3E) in MIA PaCa-2 (low NRF2 basal levels) further sensitizes the cells to gemcitabine (Fig. 2F, Supplementary Table S2F). These data collectively demonstrate NRF2's critical role in conferring chemoresistance to PDAC cells.

Assessment of metabolic signaling by activated NRF2 in PDAC cells

We next sought to determine the metabolic effects caused by NRF2 in PDAC cells. After validating the dosage of AI-1 needed to activate NRF2 pathway downstream effectors (Fig. 3A), we performed metabolomic analysis (Supplementary Fig. S4 A). Metabolite set enrichment analysis (MSEA) of upregulated metabolites revealed enrichments in protein biosynthesis, amino acid metabolism (aspartate, methionine, arginine, proline, alanine, and cysteine), ammonia recycle, urea cycle, and malate-aspartate shuttle, along with glutathione metabolism upon NRF2 activation (Fig. 3B **1st panel**). To better understand metabolic changes following NRF2 upregulation in PDAC cells, we also performed network analysis to identify key pathway clusters regulated by activated NRF2 (Fig. 3B **2nd panel,** Supplementary Fig. S4B). As expected, the amino acids pool was one of the most enriched compound clusters upon NRF2 activation in BxPC-3 cells. In addition, we sought to determine the effect that similar treatment had on lipid composition. We performed a lipidomic analysis of BxPC-3 cells upon AI-1 treatment and, except for minimal induction in triacylglycerol level, we found no other significant changes among major lipid class compositions following NRF2 activation (Fig. 3C).

We also looked at NRF2 activation's impact on cell cycle progression (Supplementary Fig. S5 A, B) by analyzing flow cytometry. We found no significant changes. We performed a time course study of AI-1 in BxPC-3 cells, and within six hours, major metabolic signaling markers were dramatically induced (Fig. 3D). A similar phenomenon occurred when we elevated NRF2 level in MIA PaCa-2 cells using a pharmacological (Fig. 3E) or genetic (Fig. 3F) approach. Oncomine analysis suggested that these metabolic genes are upregulated in human PDAC samples compared to their normal counterparts. Interestingly, analysis of TCGA PAAD datasets also suggests that those metabolic genes induced by NRF2 activation are significantly up-regulated at later stages or higher grades of pancreatic cancer (Table 1).

From our metabolomic data analysis, the common factor behind the metabolic changes appears to be glutamine metabolism. In this context, it is noteworthy that protein biosynthesis and amino acid synthesis, including other enriched pathways that were heightened upon NRF2 activation, are regulated by glutaminolysis (10). Likewise, major glutamine metabolic pathway intermediates such as GLS1, GOT1, GDH1, xCT, and GCLC were induced upon NRF2 activation (Fig. 3D-F).

We next examined the effect of NRF2 activation on the DNA damage pathway caused by gemcitabine. By measuring the levels of well-known DNA damage stress response pathway markers (28), we demonstrated that NRF2 activation can reverse DNA damage induced by gemcitabine (Fig. 3G), which establishes NRF2's comprehensive role in PDAC metabolic

signaling. These results show that activated NRF2 plays a significant role in pancreatic cancer metabolic signaling pathways.

Glutamine deprivation restricts PDAC cells proliferation and curbs chemoresistance

After exploring NRF2's role in PDAC metabolism and observing the correlation between glutamine metabolism and NRF2 upregulation, we sought to elucidate the role of metabolic pathways in gemcitabine-resistant PDAC patients. Based on Oncomine analysis, we identified the upregulation of GLS1 (glutaminase1) in gemcitabine-resistant samples (Supplementary Fig. S6A). To satisfy our curiosity, we further analyzed TCGA data for gemcitabine-treated PAAD patients and compared relative metabolic pathway enrichments between gemcitabine-treated patients with responsive and resistant groups (Supplementary TableS3, Supplementary Fig. S6B-E). It appears that higher expressions of NRF2 and GLS1 mRNA were detected in a small subset of patients grouped under gemcitabine-resistant pancreatic cancer patients, with trivial significance (Supplementary Fig. S6F). However, the nucleotide biosynthetic pathway was significantly enriched in patients with progressive disease compared with patients from complete response in patients of all stages as well as stage 2–only patients (Fig. 4A, Supplementary TableS3). Given that KRAS mediates PDAC tumor survival by regulating nucleotide synthesis (8) and that glutamine is a central precursor for protein and nucleotide biosynthesis (10,29), we theorized that targeting glutamine metabolism would enhance sensitivity to chemotherapy.

Glutaminolysis plays diverse roles in cellular metabolism. Once inside the cell, glutamine is deaminated to glutamate by GLS and then converted to α-ketoglutarate and non-essential amino acids by GOT. α-ketoglutarate plays a critical role in anaplerotic entry of glutamine into the TCA cycle. Glutamate is also exported to the extracellular space by the xCT antiporter concurrent with the exchange of cystine to support the redox balance inside the cell (10). The conversion of α-ketoglutarate from isocitrate is mediated by IDH1, whereas a multi-step conversion of heme from α-ketoglutarate (30) is followed by the generation of biliverdin mediated by HMOX1. The interplay between genes induced by activated NRF2 (indicated in Fig. 3D-F) and glutaminolysis is summarized in Fig. 4B. As expected, glutamine deprivation affects PDAC cell proliferation (Fig. 4C, Supplementary Fig. S7A), which could be rescued (Fig. 4D, Supplementary Fig. S7B) by adding glutaminolysis intermediates (α-ketoglutarate and non-essential amino acids) or by using erastin, an xCT (glutamate-cysteine antiporter) inhibitor. The combination of both α-ketoglutarate and non-essential amino acids rescued proliferation in glutamine-starved PANC-1, indicating that generating both α-ketoglutarate and non-essential amino acids in the transaminase reaction is critical for cell proliferation. These data elucidate PDAC cells' dependence on glutamine metabolism, specifically the utilization of glutamine anaplerosis in the TCA cycle and on cystine import, which occurs upon glutamate export. The ability of erastin to rescue the effect of glutamine deprivation potentiates the critical role played by cystine in glutamine dependence of PDAC cells.

To determine whether glutamine deprivation would overcome chemoresistance in PDAC, we tested the effect of glutamine limitation on a chemoresistance marker, glutathione peroxidase 4 (GPX4), that lies downstream of the glutamate-cysteine antiporter system and is also

regulated by NRF2 (31,32). By controlling glutathione synthesis, NRF2 is involved in this process (33). Surprisingly, glutamine deprivation reduced GPX4 levels (Fig. 4E). We also examined the effect of glutamine restriction on another marker of chemoresistance—stress-granule formation—which is upregulated by the production of a prostaglandin, 15d-PGJ2, in mutant KRAS cells (34,35). In agreement with earlier findings (36), we found that 15d-PGJ2 activates NRF2 and forms stress granules (Fig. 4F). We then knocked down NRF2 and observed that ablating NRF2 decreased stress-granule index (Fig. 4G), stress-granule number, and area covered by stress granules (Supplementary Fig. S7C). Therefore, 15d-PGJ2-induced stress-granule formation is controlled by NRF2 (Fig. 4H, Supplementary Fig. S7D). Remarkably, glutamine starvation restricts the capacity of 15d-PGJ2 to form stress granules in PDAC cells (Fig. 4I), which has been confirmed by decreased stress-granule number, stress-granule index, and stress-granule area upon glutamine limitation (Fig. 4J, Supplementary Fig. S7E). Consistent with a previous report (37), gemcitabine alone could not trigger stress-granule formation, but 15d-PGJ2 was able to form stress-granules under gemcitabine treatment, which could be restricted by glutamine deprivation (Fig. 4K). Taken together, our data indicate that, by perturbing glutamine metabolism, we can restrain chemoresistance in PDAC cells and control pancreatic cancer cell proliferation.

Disruption of glutamine metabolism potentiates the efficacy of gemcitabine in pancreatic cancer

Recent studies suggest that exploiting glutamine dependence could lead to new therapeutic strategies (38,39). Therefore, we evaluated the effect of glutamine starvation in combination with gemcitabine on PDAC cell survival. Glutamine starvation in combination with gemcitabine significantly reduced clonogenic survival versus gemcitabine alone (Fig. 5A). As anticipated, glutamine deprivation sensitizes PDAC cells to gemcitabine; remarkably it could be rescued by adding α-ketoglutarate and non-essential amino acids (Fig. 5B, Supplementary Fig. S8A). This signifies the role of glutamine and its contribution to nucleotide biosynthesis through anaplerotic reactions, rationalizing the sensitization of cells to gemcitabine during glutamine starvation. While combining gemcitabine with glutamine restriction, SU.86.86 cells create a synthetic lethal phenotype (Fig. 5C), a result not seen in non-cancerous cells (Fig. 5D, Supplementary Fig. S8B). Even though glutamine deprivation can be achieved in cell culture, this is clearly not a viable option *in vivo*. However, interfering with glutaminolysis is a possible approach. Various combinations of chemotherapeutic agents (such as gemcitabine; capecitabine; and 5-FU, which interferes with DNA synthesis) sensitize PDAC cells to pharmacological inhibitors (glutaminase inhibitors: CB-839, BPTES) of glutamine metabolism (Fig. 5E). Next, we examined the impact of a potent GPX4 inhibitor, RSL3, in PANC-1 cells and found that enhanced gemcitabine sensitivity was detected after adding RSL3 (Fig. 5F). Since both glutamine metabolism and NRF2 affect GPX4, we checked the effect of a GPX4 inhibitor on gemcitabine sensitivity in PDAC cells. These data suggest that NRF2 and glutaminolysis regulate chemoresistance in conjunction with GPX4. Notably, some of these small molecule agents targeting metabolism are approved or involved in clinical trials for the treatment of cancer patients (40). To evaluate the combination of a glutaminase inhibitor, CB-839, with gemcitabine in PDAC *in vivo*, we followed the drug treatment dosing scheme shown in Fig. 5G. This scheme is used in multiple preclinical models of pancreatic ductal adenocarcinoma,

including the genetically engineered KPC mice allograft model of PDA (Fig. 5H-I), MIA PaCa-2 (Fig. 5J-K), SU.86.86 (Fig. 5L-M), and PANC-1 (Fig. 5N-O) cell-xenograft model. This combination caused tumor regression (Fig. 5H, 5J, 5L, 5N) without adverse events or marked differences in mean body weight (Fig. 5I, 5K, 5M, 5O). While it was important to examine the effect of treatments on NRF2 level in *in vivo* models, we could not detect any significant changes in NRF2 expression upon combination therapies in MIA PaCa-2 and PANC-1 xenograft models (Supplementary Fig. S8C-D). Kaplan-Meier analysis shows that this drug combination has significant anti-tumor effects. And, while neither CB-839 nor gemcitabine alone impacted survival, we found that the combination notably improved median survival over vehicle-treated animals or any single-drug-treated cohort (Fig. 5P). CB-839 is being used in clinical trials for multiple cancers, including in combination with another chemotherapeutic agent (capecitabine: NCT02861300), and it is ready for a basket trial in patients with NRF2 aberrant tumors (41). Our finding (summarized in Fig. 6) that disrupting glutamine metabolism potentiates the efficacy of chemotherapy represents an attractive approach to treating RAS-driven pancreatic cancer patients.

DISCUSSION

In PDAC cells, mutant KRAS transcriptionally activates NRF2, a principal modulator of cellular redox, resulting in a reduced intracellular environment (42). NRF2 is also activated following MAPK inhibitor treatment, suggesting a role for NRF2 in RAS pathway drug sensitivity (14,43). Recently, Papagiannakopoulos and colleagues (20,44) reported that hyperactivation of NRF2 leads to increased glutamine dependency. Our data, which confirm these reports, show the induction of key proteins involved in glutamine metabolism following NRF2 upregulation in PDAC cells. Interestingly, some of those upregulated signaling nodes are associated with PDAC chemoresistance (45), suggesting that targeting glutamine metabolism could be an effective strategy to combat chemoresistance. Although activated NRF2 was not identified as a predictive marker, our data indicate that the NRF2-driven metabolic state makes PDAC cells sensitive to glutaminase inhibition, which is not validated in NRF2-low cells as they are also sensitive to CB-839. While other factors independent of NRF2 level (13,34,46) could influence sensitivity to the CB-839-gemcitabine combination in KRAS-mutant NRF2-low cells, it is also possible that NRF2 and KRAS regulate a convergent set of metabolic pathways such that NRF2 provides an additional benefit to NRF2-high cells and imparts glutaminase dependency. Further studies in GEM models of PDAC will be required to understand the complex mechanism of gemcitabine sensitivity with glutaminase inhibition in KRAS-driven PDAC cells specifically in the light of variable NRF2 level.

In addition to activating the NRF2 detoxification system, oncogenic KRAS alters glucose and glutamine metabolism to support PDAC cell proliferation (1,9). Glutamine is a critical nutrient for cell growth and survival. It supports cell proliferation with the necessary intermediates for biosynthesis by providing carbon and nitrogen backbones for nucleotide and amino acid synthesis (10,29). Interestingly, our data indicate that the production of non-essential amino acids along with α-ketoglutarate is critical for cell growth, whereas cystine import at the expense of glutamate also plays a significant role in PDAC cell proliferation. Surprisingly, we found that glutamine restriction not only affects PDAC cell proliferation but

also regulates the level of GPX4, a protein responsible for cancer cell survival during therapeutic treatment (47). It has also been reported that GPX4 is transcriptionally modulated by NRF2 and is regulated by glutathione metabolism (31,32). Our data demonstrating downregulation of GPX4 upon glutamine restriction signify the impact of targeting glutaminolysis to combat chemoresistance. Recent work from the Vander-Heiden group revealed that cancer cells' glutamine dependence is driven by xCT in combination with physiological concentration of cystine (46). Consistent with their findings, our data suggest that activated NRF2 induces xCT to increase glutamine dependence, signifying xCT's role in facilitating the effects of glutamine restriction in PDAC cells.

We also found that a glutamine deficit can constrain the assembly of stress granules, which form in response to chemotherapy and in turn provide cyto-protection against stress stimuli (37,48). A recent study revealed that KRAS upregulates stress-granule formation, which contributes to chemoresistance. Mutant KRAS induces 15-d-PGJ2 accumulation, which mediates upregulated stress-granule formation, and KRAS-dependent stress-granule induction confers chemotherapy resistance (34). Prostaglandin 15-d-PGJ2 is known to induce the antioxidant system that regulates NRF2-mediated pathway activation (36,49). Here we report that glutamine restriction reduces the capacity of 15-d-PGJ2 to form stress granules in KRAS-driven PDAC cells. Future studies of glutamine metabolism's role in regulating 15-d-PGJ2-mediated NRF2 antioxidant pathway activation and cytoprotective stress-granule accumulation will elucidate the complexity of chemoresistance in KRAS-mutant cancer cells.

We have observed that perturbing glutamine metabolism reinforces chemotherapy treatment and shown that a first-in-class small molecule glutaminase inhibitor, CB-839, which is currently in a Phase II clinical trial (NCT03263429), enhances the efficacy of gemcitabine and that this combination enhances tumor regression in a mouse model. Importantly, the doses used in this combination treatment are clinically tolerated. In addition, combining CB-839 with gemcitabine shows that utilizing chemotherapy could mitigate the adaptiveness of PDAC towards glutamine metabolism, substantiating recent findings from Kimmelman and colleagues (38). Consistent with their report, we demonstrated that glutaminase inhibition combined with chemotherapy delays tumor growth, even though single treatments of CB-839 or gemcitabine were ineffective. By using multiple preclinical models including KPC allograft and three different xenograft models, we have provided evidence that interfering with glutamine metabolism could overcome resistance against chemotherapies, suggesting that a clinical trial using this combinatorial therapy is merited in pancreatic cancer patients. While our preclinical studies are encouraging and equally promising, they are preliminary in nature given their dependence on subcutaneous xenografts and allograft models. Though those models were employed as the first step in validating cell-line results, which allowed for rapid screening to asses safety and efficacy of drug combinations, they have limitations. These include exhibiting a less-functional immune system, displaying a poor microenvironment, and lacking cellular diversity (50). Notably, a differential functional dependence on glutamine metabolism in variable environmental contexts has been indicated recently (46). Future work in genetically engineered PDAC mouse models will more adequately reflect the clinical application of this combination treatment.

Overcoming resistance to existing therapies is one of the major challenges for PDAC patient treatment. By combining glutamine metabolism inhibitors with chemotherapeutic drugs, we exploit the reliance of PDAC on glutamine and increased glutamine dependency upon NRF2 activation (Fig. 6). This study highlights therapeutic opportunities created by the metabolic reprogramming liability in pancreatic cancer cells and provides a possible therapeutic intervention for chemoresistant pancreatic cancer patients. Future studies exploring this finding in a larger clinical context are warranted. It is conceivable that the metabolic needs associated with KRAS could be exploited to overcome chemotherapy resistance in a wide array of RAS-driven pancreatic cancers.

Supplementary Material

Refer to Web version on PubMed Central for supplementary material.

Acknowledgement

We thank Drs. Elda Grabocka, Jefferson University, for sharing details on stress granule assay, Gina M. DeNicola, Moffitt Cancer Center, for providing technical advice with NRF2 shRNAs and NRF2 antibody optimizations, and Pankaj K. Singh, Eppley Institute, for kindly sharing the gemcitabine treated stage II pancreatic cancer patients classification TCGA metafile. We thank Dr. Sung Eun Kim/UCSF for critical reading of the manuscript. We would like to thank Dr. Brynmor A. Watkins/Pharma Models, LLC for assistance with the mouse study, Allan Wang/US Biomax for assistance with the TMA study, and Sili Fan/UC Davis for assistance with metabolomic data analysis. We also would like to thank members of the Frederick National Laboratory (Drs. Carissa Grose, Oscar Cheng, Robert Stephens), NCI SPGM, NIH West Coast Metabolomics Center, and Lipotype GmbH for their technical assistance.

Financial Support: This work was supported by grants from the National Cancer Institute, HHS-National Institutes of Health, under Contract No. HHSN261200800001E. The content of this publication does not necessarily reflect the views or policies of the Department of Health and Human Services (HHS), nor does mention of trade names, commercial products, or organizations imply endorsement by the U.S. Government.

REFERENCES:

1. Sousa CM, Kimmelman AC. The complex landscape of pancreatic cancer metabolism. Carcinogenesis 2014;35:1441–50 [PubMed: 24743516]
2. Grasso C, Jansen G, Giovannetti E. Drug resistance in pancreatic cancer: Impact of altered energy metabolism. Crit Rev Oncol Hematol 2017;114:139–52 [PubMed: 28477742]
3. Oberstein PE, Olive KP. Pancreatic cancer: why is it so hard to treat? Therap Adv Gastroenterol 2013;6:321–37
4. Bryant KL, Mancias JD, Kimmelman AC, Der CJ. KRAS: feeding pancreatic cancer proliferation. Trends Biochem Sci 2014;39:91–100 [PubMed: 24388967]
5. McCormick F KRAS as a Therapeutic Target. Clin Cancer Res 2015;21:1797–801 [PubMed: 25878360]
6. Pavlova NN, Thompson CB. The Emerging Hallmarks of Cancer Metabolism. Cell Metab 2016;23:27–47 [PubMed: 26771115]
7. Hanahan D, Weinberg RA. Hallmarks of cancer: the next generation. Cell 2011;144:646–74 [PubMed: 21376230]
8. Santana-Codina N, Roeth AA, Zhang Y, Yang A, Mashadova O, Asara JM, et al. Oncogenic KRAS supports pancreatic cancer through regulation of nucleotide synthesis. Nat Commun 2018;9:4945 [PubMed: 30470748]
9. White E Exploiting the bad eating habits of Ras-driven cancers. Genes Dev 2013;27:2065–71 [PubMed: 24115766]
10. Altman BJ, Stine ZE, Dang CV. From Krebs to clinic: glutamine metabolism to cancer therapy. Nat Rev Cancer 2016;16:749 [PubMed: 28704361]

11. Halbrook CJ, Lyssiotis CA. Employing Metabolism to Improve the Diagnosis and Treatment of Pancreatic Cancer. Cancer Cell 2017;31:5–19 [PubMed: 28073003]
12. Toda K, Nishikawa G, Iwamoto M, Itatani Y, Takahashi R, Sakai Y, et al. Clinical Role of ASCT2 (SLC1A5) in KRAS-Mutated Colorectal Cancer. Int J Mol Sci 2017;18
13. Son J, Lyssiotis CA, Ying H, Wang X, Hua S, Ligorio M, et al. Glutamine supports pancreatic cancer growth through a KRAS-regulated metabolic pathway. Nature 2013;496:101–5 [PubMed: 23535601]
14. DeNicola GM, Karreth FA, Humpton TJ, Gopinathan A, Wei C, Frese K, et al. Oncogene-induced Nrf2 transcription promotes ROS detoxification and tumorigenesis. Nature 2011;475:106–9 [PubMed: 21734707]
15. Tao S, Wang S, Moghaddam SJ, Ooi A, Chapman E, Wong PK, et al. Oncogenic KRAS confers chemoresistance by upregulating NRF2. Cancer Res 2014;74:7430–41 [PubMed: 25339352]
16. Takahashi N, Chen HY, Harris IS, Stover DG, Selfors LM, Bronson RT, et al. Cancer Cells Co-opt the Neuronal Redox-Sensing Channel TRPA1 to Promote Oxidative-Stress Tolerance. Cancer Cell 2018;33:985–1003 e7 [PubMed: 29805077]
17. Hayes JD, Dinkova-Kostova AT. The Nrf2 regulatory network provides an interface between redox and intermediary metabolism. Trends Biochem Sci 2014;39:199–218 [PubMed: 24647116]
18. Rojo de la Vega M, Chapman E, Zhang DD. NRF2 and the Hallmarks of Cancer. Cancer Cell 2018;34:21–43 [PubMed: 29731393]
19. Mitsuishi Y, Taguchi K, Kawatani Y, Shibata T, Nukiwa T, Aburatani H, et al. Nrf2 redirects glucose and glutamine into anabolic pathways in metabolic reprogramming. Cancer Cell 2012;22:66–79 [PubMed: 22789539]
20. Sayin VI, LeBoeuf SE, Singh SX, Davidson SM, Biancur D, Guzelhan BS, et al. Activation of the NRF2 antioxidant program generates an imbalance in central carbon metabolism in cancer. Elife 2017;6
21. Mukhopadhyay S, Saqcena M, Chatterjee A, Garcia A, Frias MA, Foster DA. Reciprocal regulation of AMP-activated protein kinase and phospholipase D. J Biol Chem 2015;290:6986–93 [PubMed: 25632961]
22. Tadros S, Shukla SK, King RJ, Gunda V, Vernucci E, Abrego J, et al. De Novo Lipid Synthesis Facilitates Gemcitabine Resistance through Endoplasmic Reticulum Stress in Pancreatic Cancer. Cancer Res 2017;77:5503–17 [PubMed: 28811332]
23. Satoh H, Moriguchi T, Takai J, Ebina M, Yamamoto M. Nrf2 prevents initiation but accelerates progression through the Kras signaling pathway during lung carcinogenesis. Cancer Res 2013;73:4158–68 [PubMed: 23610445]
24. Matzinger M, Fischhuber K, Heiss EH. Activation of Nrf2 signaling by natural products-can it alleviate diabetes? Biotechnol Adv 2018;36:1738–67 [PubMed: 29289692]
25. Zhang M, Wu YQ, Xie L, Wu J, Xu K, Xiao J, et al. Isoliquiritigenin Protects Against Pancreatic Injury and Intestinal Dysfunction After Severe Acute Pancreatitis via Nrf2 Signaling. Front Pharmacol 2018;9:936 [PubMed: 30174606]
26. Ju HQ, Gocho T, Aguilar M, Wu M, Zhuang ZN, Fu J, et al. Mechanisms of Overcoming Intrinsic Resistance to Gemcitabine in Pancreatic Ductal Adenocarcinoma through the Redox Modulation. Mol Cancer Ther 2015;14:788–98 [PubMed: 25527634]
27. Hur W, Sun Z, Jiang T, Mason DE, Peters EC, Zhang DD, et al. A small-molecule inducer of the antioxidant response element. Chem Biol 2010;17:537–47 [PubMed: 20534351]
28. Bartek J, Lukas J. Chk1 and Chk2 kinases in checkpoint control and cancer. Cancer Cell 2003;3:421–9 [PubMed: 12781359]
29. DeBerardinis RJ, Cheng T. Q's next: the diverse functions of glutamine in metabolism, cell biology and cancer. Oncogene 2010;29:313–24 [PubMed: 19881548]
30. Rouault TA. Heme, whence come thy carbon building blocks? Blood 2018;132:981–2 [PubMed: 30190349]
31. Stockwell BR, Friedmann Angeli JP, Bayir H, Bush AI, Conrad M, Dixon SJ, et al. Ferroptosis: A Regulated Cell Death Nexus Linking Metabolism, Redox Biology, and Disease. Cell 2017;171:273–85 [PubMed: 28985560]

32. Abdalkader M, Lampinen R, Kanninen KM, Malm TM, Liddell JR. Targeting Nrf2 to Suppress Ferroptosis and Mitochondrial Dysfunction in Neurodegeneration. Front Neurosci 2018;12:466 [PubMed: 30042655]
33. Kong H, Chandel NS. Regulation of redox balance in cancer and T cells. J Biol Chem 2018;293:7499–507 [PubMed: 29282291]
34. Grabocka E, Bar-Sagi D. Mutant KRAS Enhances Tumor Cell Fitness by Upregulating Stress Granules. Cell 2016;167:1803–13 e12 [PubMed: 27984728]
35. Anderson P, Kedersha N, Ivanov P. Stress granules, P-bodies and cancer. Biochim Biophys Acta 2015;1849:861–70 [PubMed: 25482014]
36. Kansanen E, Kivela AM, Levonen AL. Regulation of Nrf2-dependent gene expression by 15-deoxy-Delta12,14-prostaglandin J2. Free Radic Biol Med 2009;47:1310–7 [PubMed: 19573595]
37. Kaehler C, Isensee J, Hucho T, Lehrach H, Krobitsch S. 5-Fluorouracil affects assembly of stress granules based on RNA incorporation. Nucleic Acids Res 2014;42:6436–47 [PubMed: 24728989]
38. Biancur DE, Paulo JA, Malachowska B, Quiles Del Rey M, Sousa CM, Wang X, et al. Compensatory metabolic networks in pancreatic cancers upon perturbation of glutamine metabolism. Nat Commun 2017;8:15965 [PubMed: 28671190]
39. Mukhopadhyay S, Saqcena M, Foster DA. Synthetic lethality in KRas-driven cancer cells created by glutamine deprivation. Oncoscience 2015;2:807–8 [PubMed: 26682255]
40. Luengo A, Gui DY, Vander Heiden MG. Targeting Metabolism for Cancer Therapy. Cell Chem Biol 2017;24:1161–80 [PubMed: 28938091]
41. Sen S, Hess KR, Roszik J, Shaw KR, Heymach J, Huang L, et al. Characterization of KEAP1-NRF2 genomic alterations across diverse tumor types: Co-occurring alterations, survival outcomes, and implications for targeting cancer metabolism. 2018;36:2558-
42. Chio IIC, Jafarnejad SM, Ponz-Sarvise M, Park Y, Rivera K, Palm W, et al. NRF2 Promotes Tumor Maintenance by Modulating mRNA Translation in Pancreatic Cancer. Cell 2016;166:963–76 [PubMed: 27477511]
43. Krall EB, Wang B, Munoz DM, Ilic N, Raghavan S, Niederst MJ, et al. KEAP1 loss modulates sensitivity to kinase targeted therapy in lung cancer. Elife 2017;6
44. Romero R, Sayin VI, Davidson SM, Bauer MR, Singh SX, LeBoeuf SE, et al. Keap1 loss promotes Kras-driven lung cancer and results in dependence on glutaminolysis. Nat Med 2017;23:1362–8 [PubMed: 28967920]
45. Gebregiworgis T, Bhinderwala F, Purohit V, Chaika NV, Singh PK, Powers RJM. Insights into gemcitabine resistance and the potential for therapeutic monitoring. 2018;14:156
46. Muir A, Danai LV, Gui DY, Waingarten CY, Lewis CA, Vander Heiden MG. Environmental cystine drives glutamine anaplerosis and sensitizes cancer cells to glutaminase inhibition. Elife 2017;6
47. Hangauer MJ, Viswanathan VS, Ryan MJ, Bole D, Eaton JK, Matov A, et al. Drug-tolerant persister cancer cells are vulnerable to GPX4 inhibition. Nature 2017;551:247–50 [PubMed: 29088702]
48. Mahboubi H, Stochaj U. Cytoplasmic stress granules: Dynamic modulators of cell signaling and disease. Biochim Biophys Acta Mol Basis Dis 2017;1863:884–95 [PubMed: 28095315]
49. Kim EH, Surh YJ. 15-deoxy-Delta12,14-prostaglandin J2 as a potential endogenous regulator of redox-sensitive transcription factors. Biochem Pharmacol 2006;72:1516–28 [PubMed: 16987499]
50. Saluja AK, Dudeja V. Relevance of animal models of pancreatic cancer and pancreatitis to human disease. Gastroenterology 2013;144:1194–8 [PubMed: 23622128]

STATEMENT OF SIGNIFICANCE

Findings illuminate the mechanistic features of KRAS-mediated chemoresistance and provide a rationale for exploiting metabolic reprogramming in pancreatic cancer cells to confer therapeutic opportunities that could be translated into clinical trials.

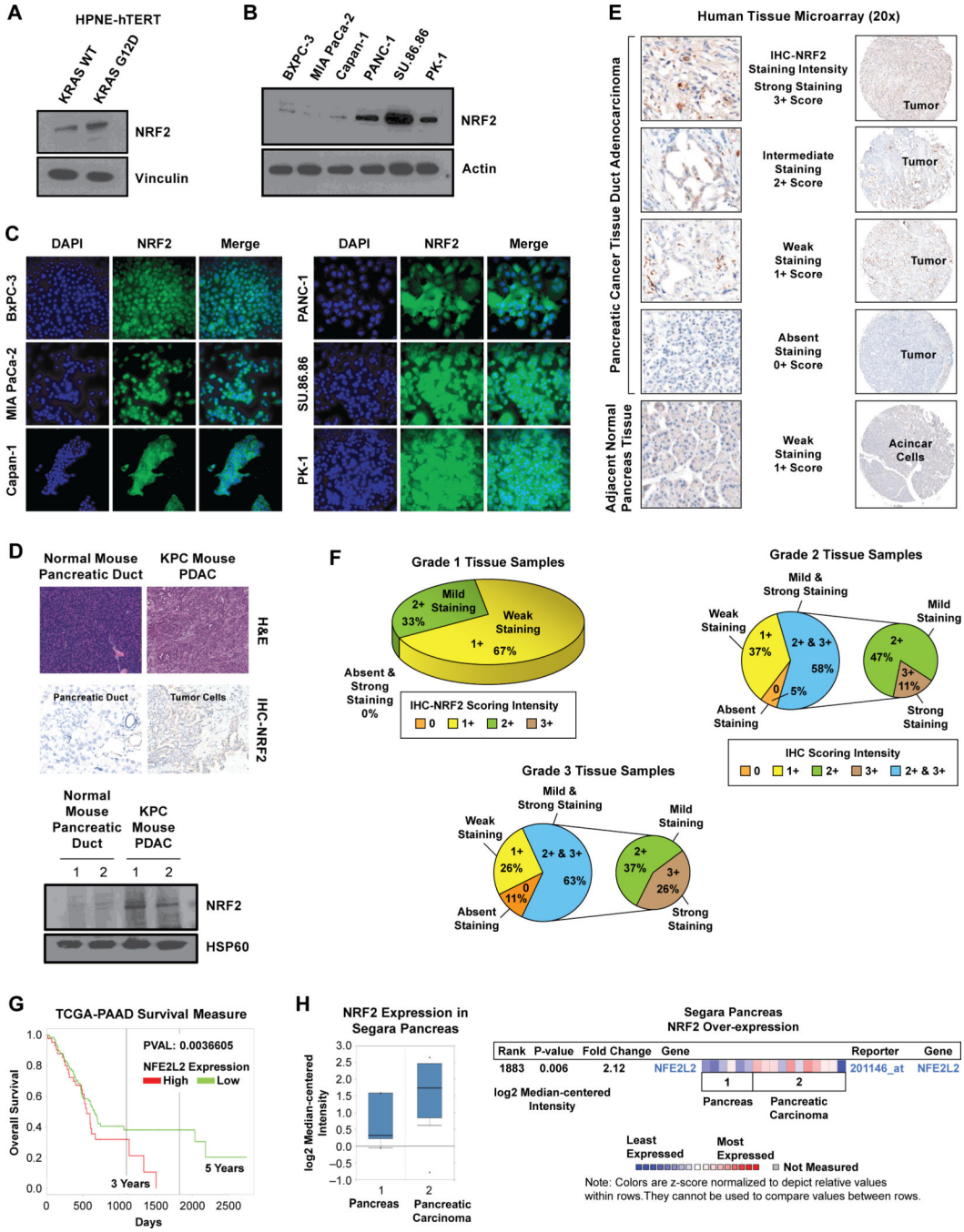

Figure 1. Differential expression of NRF2 in pancreatic cancer.

A, Western blot showing the basal level of NRF2 in HPNE-hTERT KRAS WT and KRAS G12D cells. Vinculin is the loading control. **B,** NRF2 basal level detected by western blot in PDAC, BxPC-3, MIA Paca-2, Capan-1, PANC-1, SU.86.86, and PK-1 cells. Actin is the loading control. **C,** Immunofluorescence staining of NRF2 (green) in PDAC cells. Blue, DAPI-stained nuclei. Images are in 40x view, scale bars 20 μm **D,** Normal and KPC mouse pancreatic ductal tissue sections were processed for (upper panel) western blotting and (lower panel) H&E staining (top), immunohistochemical (bottom) staining for NRF2 (20x

view). Scale bars, 200 μm for images. Hsp60 is the loading control in western blot. Representative data (A-D) are shown from at least two independent experiments. **E,** Representative images of immunohistological staining of NRF2 in a human tissue microarray of the pancreas showing absent (0+), weak (1+), intermediate (2+), and strong (3+) staining intensity. Images are in 20x view, scale bars 100μm (left), 2mm (right). **F,** Pie charts generated for each grade of tissue sample based on NRF2 staining intensity. Immunohistochemical scoring intensity was classified with the indicated colors. The relative distribution of each group was normalized to the total number of each grade of tissue sample and given a value of 100%. **G,** Survival analysis for TCGA-PAAD was bifurcated at the 75th percentile and grouped by high versus low levels of NFE2L2 gene expression. **H,** Oncomine analysis depicts the elevated expression of NRF2 at the mRNA level in human pancreatic cancers compared to normal pancreatic tissues.

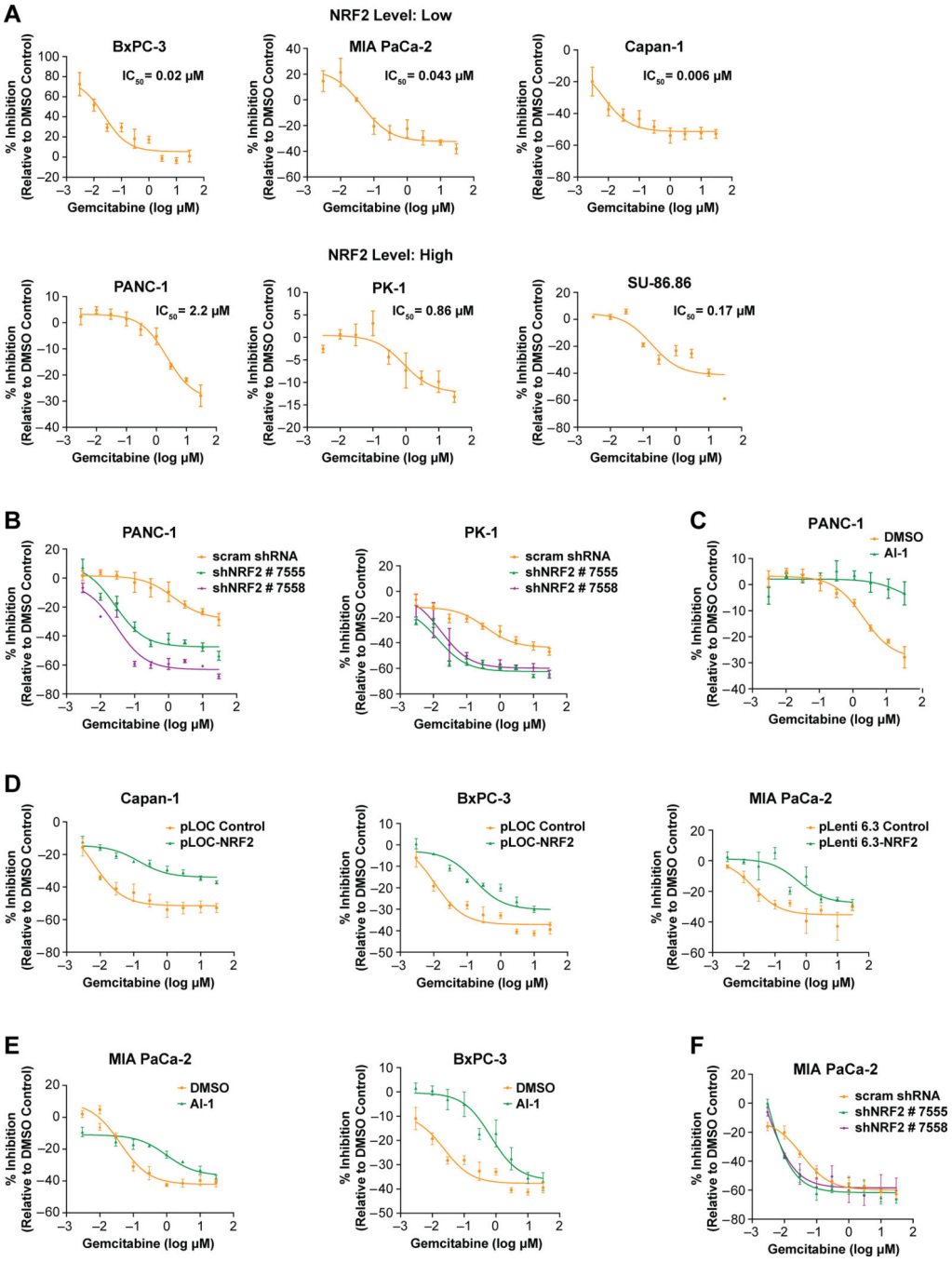

Figure 2. NRF2 mediates chemoresistance in PDAC cells:

A, PDAC cells were treated with increasing concentrations of gemcitabine for 48 hours. Percentage of drug inhibition was determined using the CellTiter-Glo assay. IC50 values were determined using GraphPad Prism. **B,** PANC-1 and PK-1 cells were transiently transfected with shRNA expression vectors targeting NRF2 or scrambled on seeding day. Titrations of gemcitabine were treated on the following day. Drug inhibition percentage was calculated as in A. **C,** PANC-1 cells were treated with 10 μM AI-1 and increasing doses of gemcitabine or DMSO control for 48 hours. **D,** Stable cells with NRF2 over-expressing

Capan-1 and BxPC-3 were treated by nine-point gemcitabine titration for 48 hours to analyze drug inhibition percentage. MIA PaCa-2 cells were transiently transfected with NRF2 over-expressing vector or empty vector and, on the following day, treated with gemcitabine titration for 48 hours. **E,** MIA PaCa-2 and BxPC-3 cells were treated with 10 μM AI-1 and increasing doses of gemcitabine or DMSO control for 48 hours. **F,** MIA PaCa-2 cells were transiently transfected with shRNA expression vectors, and titrations of gemcitabine were treated as in B. Percent of gemcitabine inhibition was assessed by CellTiter-Glo assay and was determined relative to the proportion of respective control. Error bars represent standard error of mean (SEM) from three independent experiments.

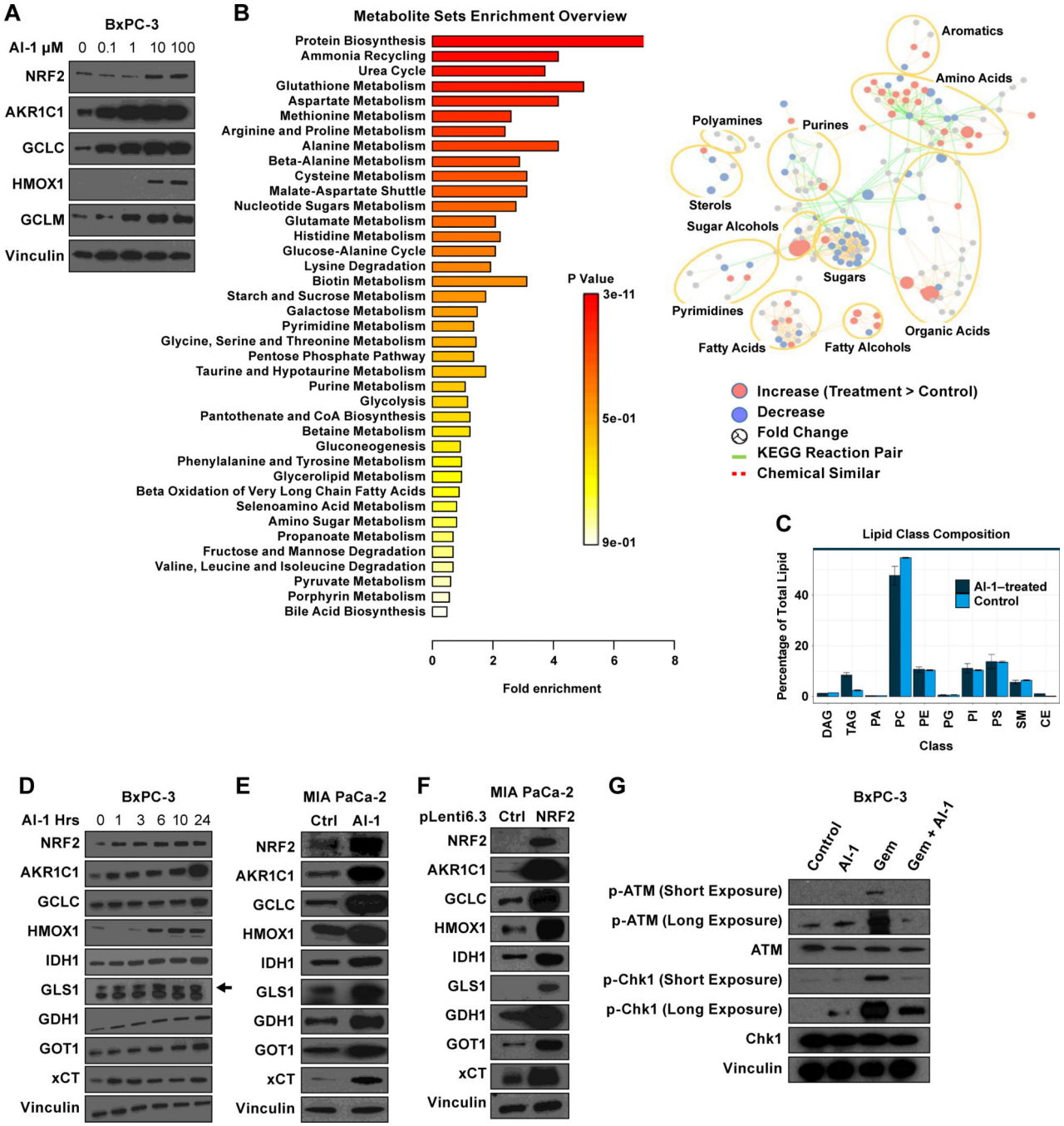

Figure 3. Effects of NRF2 activation on metabolic signaling:

A, BxPC-3 cells were dose-dependently treated with AI-1 for 24 hours. Whole cell lysates were analyzed via western blot for indicated proteins. **B,** BxPC-3 cells were treated with AI-1 (10μM, 6 hours) and subjected to metabolomic analysis by GC-TOF MS. Metabolite Set Enrichment Analysis (MSEA) of AI-1-treated BxPC-3 cells compared to their DMSO control. (left panel) Summary plots for MSEA are ranked by p-value. ($p<0.05$, Student's *t* test, n=4). (right panel) Network representation of overlapping enriched compound cluster in AI-1-treated BxPC-3 cells compared to DMSO control. Each circle represents a compound

set. Circle size corresponds to compound set size and intensity to degree of overlap. Red is upregulated and blue is downregulated. Cellular compounds associated with compound sets are listed. **C,** Bar graph illustrating the qualitative description of lipids class composition measured in AI-1-treated (10μM, 6 hours) and DMSO control of BxPC-3 cells. n=3, averages ± standard deviation. Lipid class amounts were normalized to the total lipid amount, yielding the percent of total lipids. **D,** BxPC-3 cells were treated with AI-1 (10μM) in a time-course manner and analyzed via western blot for indicated proteins. **E,** MIA PaCa-2 cells were treated with AI-1 (10μM, 24 hours) or DMSO (control) and processed for immunoblotting as in D. **F,** MIA PaCa-2 cells were transiently transfected with NRF2 over-expressing plasmid or empty backbone (p Lenti6.3) as control. Immunoblotting was performed as in E. **G,** BxPC-3 cells were treated with AI-1 (10μM) and/or gemcitabine (20ηM) for 48 hours, and indicated proteins were analyzed by immunoblotting. **A, D-G,** Vinculin is the loading control. Images are representative of at least two independent experiments.

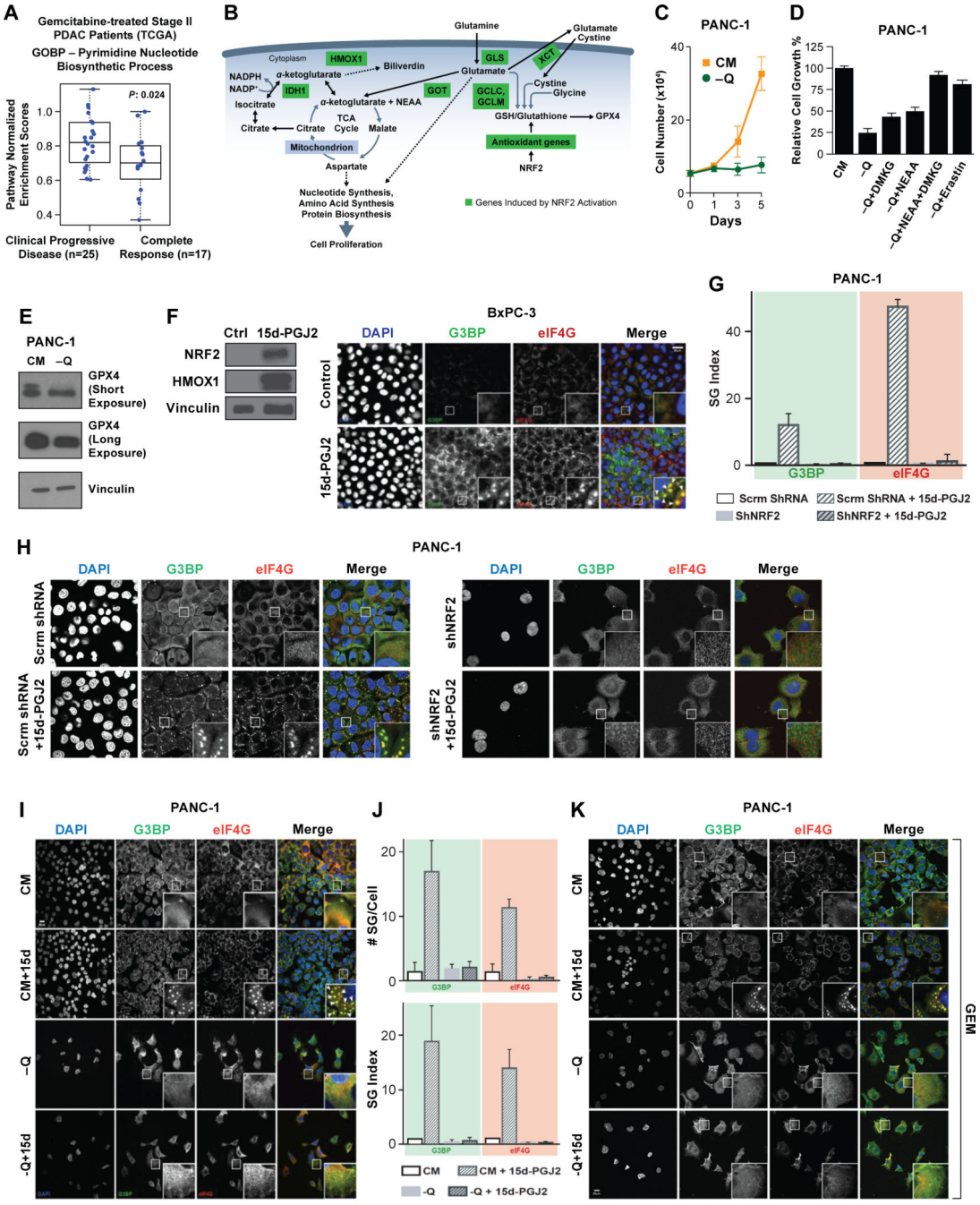

Figure 4. Effects of glutamine deprivation on cell growth and stress granule formation:

A, Nucleotide biosynthetic pathway enrichment score for gemcitabine-treated PAAD patients was determined using GOBP database. Significant p value was evaluated. **B,** Schematic overview of glutamine utilization in cancer cells and role of NRF2 in metabolism. Glutamine contributes to nucleotide biosynthesis directly or through the TCA cycle. The aspartate generated by the TCA cycle is critical for amino acid and protein biosynthesis, which in turn regulates cell proliferation. NRF2 mediates nucleotide synthesis, which in turn supports cell growth . Genes upregulated by activated NRF2 are indicated by green color. **C,**

Cells were plated in complete media (CM) containing 10% serum. After 24 hours (day 1), cells were shifted to CM or medium lacking glutamine (-Q), harvested at indicated times, and quantified after crystal violet staining. Error bars represent the SEM for three independent experiments. **D,** PANC-1 cells were plated and shifted to CM or media lacking Q, as in B. Cells were additionally treated with (5mM) DMKG, (1X) NEAA mixture, or the combination following glutamine withdrawal. For Erastin treatment, cells were shifted to Q lacking media after overnight pretreatment with 500ηM Erastin. Following indicated treatments for five days, cell proliferation was assessed as in B. Error bars represent SEM of four independent experiments. Data presented as relative percent to CM-treated condition as control. **E,** GPX4 protein levels in PANC-1 cells treated with CM or -Q for 72 hours were assessed by immunoblotting. Vinculin is the loading control. A representative image is shown from at least three independent experiments. **F,** BxPC-3 cells were treated with 15d-PGJ2 (50μM, 1 hour) or vehicle control. (left panel) Whole cell lysates were subjected to immunoblotting with indicated antibodies. Vinculin is the loading control. (right panel) Stress granules (SG) were detected by G3BP (green) and eIF4G (red) immunofluorescence staining. Blue, DAPI-stained nuclei. Scale bars, 20μm. **G,** PANC-1 cells were transiently transfected with scrambled or NRF2 shRNA as indicated. 15d-PGJ2 were treated and SGs were detected as in E. SGs were quantified by defining an SG index (SG area/cell area) based on G3BP (green) and eIF4G (red) immunofluorescence. Error bars indicate SEM for two independent experiments. **H,** PANC-1 cells were treated as in G, and SGs were detected as in F. **F-H,** The images are representative of at least two independent experiments. **I,** PANC-1 cells were plated and shifted to CM or -Q for 72 hours then treated with 15d-PGJ2 where indicated. 15d-PGJ2 treatment and SG detection were done as in F. **J,** SGs were quantified from H by number of SGs per cell and by defining an SG index as in G. Error bars indicate SEM for three independent experiments. **K,** PANC-1 cells were treated as in I. Additionally, gemcitabine (2μM, 24 hour) was added to each sample, and SGs were detected as in F. **I-K,** The images are representative of at least three independent experiments. **F,H,I,K,** Images are in 40x view, scale bars represent 20 μm.

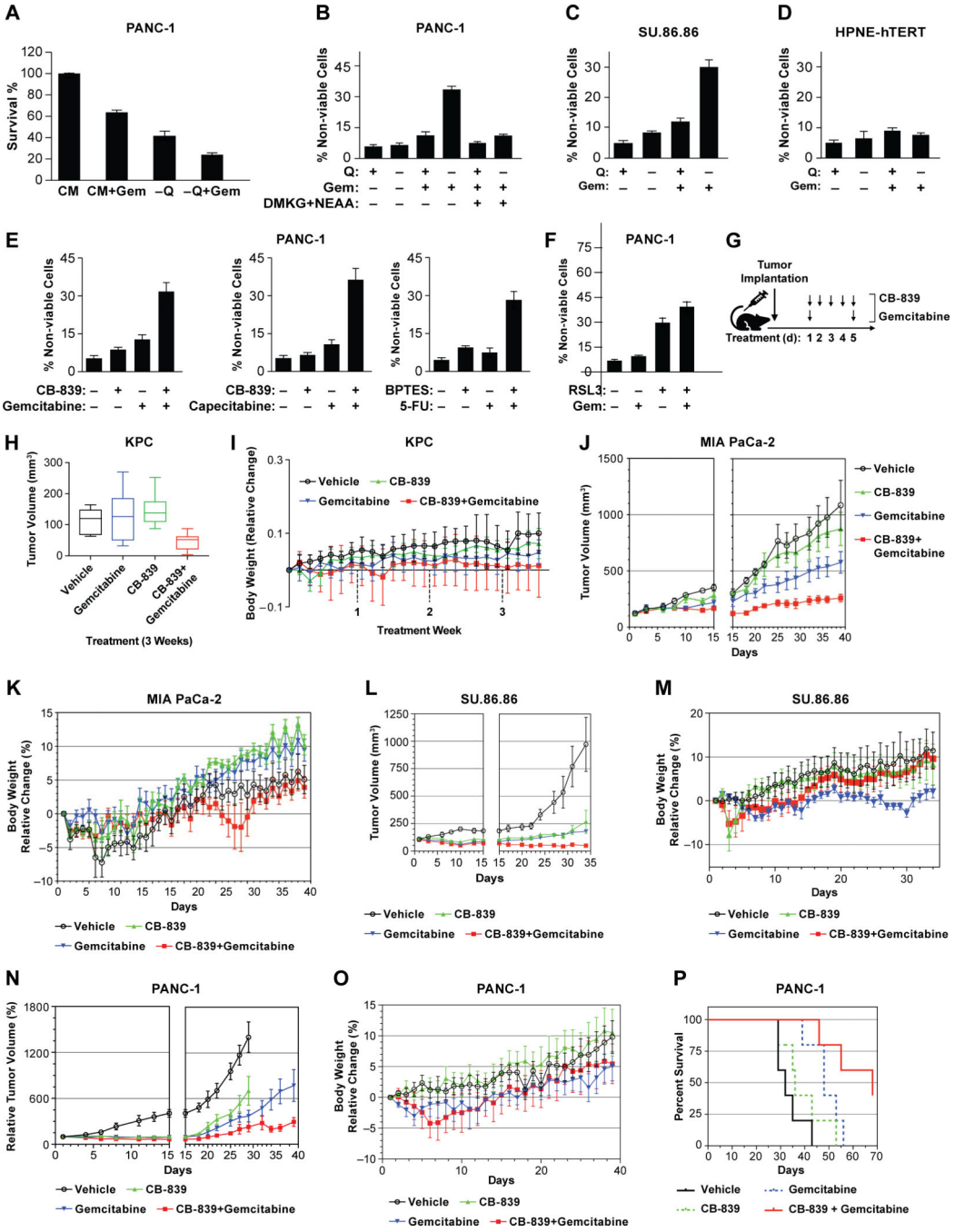

Figure 5. Disruption of glutaminolysis sensitizes PDAC cells to chemotherapeutic drugs:

A, Survival of PANC-1 cells pre-treated with CM or -Q for 72 hours followed by 36-hour gemcitabine (2μM) treatment as indicated. Values were normalized to cell survival in CM-treated condition as control, which were given a value of 100%. B, PANC-1 cells were plated and shifted to CM or media lacking Q. Cells were additionally treated with a combination of (5mM) DMKG and (1X) NEAA mixture for 72 hours following glutamine withdrawal where indicated. Gemcitabine (2μM, 36 hours) was added for respective samples, and the percent of non-viable cells was calculated using the trypan blue dye

exclusion assay. C, SU.86.86 cells were plated and treated with no glutamine media as in A. Cells were treated with 0.2μM gemcitabine for the last 24 hours as indicated, and the percent of non-viable cells was calculated. D, One day after plating, HPNE-hTERT cells were shifted to CM or medium lacking Q for 48 hours then treated with or without (2μM) gemcitabine for an additional 24 hours in the presence of pretreatment as indicated. The percent of non-viable cells was determined. E, PANC-1 cells were plated in CM overnight, after which cells were treated with 10μM CB-839 or 10μM BPTES for 72 hours where indicated. An additional treatment of 2μM capecitabine, 2μM gemcitabine, or 10μM 5-FU was given for 36 hours as indicated. The percent of non-viable cells was determined. F, PANC-1 cells were treated with RSL3 (10ηM) and/or gemcitabine (2μM) for 24 hours. The percent of non-viable cells was determined as in B. A-F, Error bars represent the SEM for four independent experiments. G, Experimental design for H-P. H-O, Mice bearing tumors of KPC (H-I), MIA PaCa-2 (J-K), SU.86.86 (L-M) and PANC-1 cells (N-O) were administered drug schedules as indicated in the schematic representation G. Tumor volumes (H, J, L, N) and body weights of mice (I, K, M, O) were shown with error bars representing SEM for each group. Threshold for p-value was <0.05. P, Survival of PANC-1 tumor-bearing mice represented as a Kaplan-Meier plot. H-P, Statistical differences between treatment groups were determined with a critical p value of <0.05. Synergistic effect of CB-839+Gemcitabine is evident by comparing tumor volumes (H,J,L,N) with single compound treated groups with statistical significance whereas insignificant body weight changes has been documented (I,K,M,O) for either of four treatment groups in all cases.

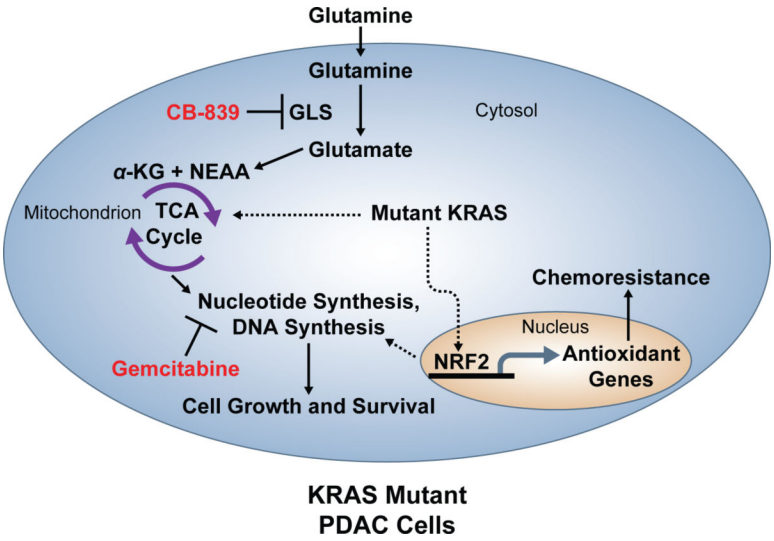

Figure 6. Perturbing glutamine metabolism potentiates the efficacy of chemotherapy in KRAS-driven pancreatic cancers:

Model illustrates reprogrammed metabolic pathways in RAS-driven PDAC cells linked to KRAS mutation and NRF2 activation, which drive glutaminolysis. Mutant KRAS-mediated NRF2 activation leads to chemoresistance by regulating antioxidant genes. Modulation of nucleotide synthesis by NRF2 also supports PDAC cell growth. Anaplerotic glutamine utilization is a key feature of KRAS-driven PDAC cells. KRAS-regulated glutamine metabolic rewiring influenced the TCA cycle, which is critical for nucleotide and DNA synthesis to support cell growth and survival (12,29). CB-839 inhibits GLS, whereas gemcitabine blocks DNA synthesis. This model potentiates CB-839 treatment along with gemcitabine as a therapeutic strategy to combat chemoresistance in KRAS-driven pancreatic cancers.

Table 1.

Upregulated expression of metabolic genes in patients with pancreatic cancer

Upregulated Expression of Metabolic Genes in Pancreatic Cancer Patients

Gene Name	Source	*P* Values (Threshold) Compared to Normal Type	Cancer Type
NRF2	TCGA	8.52E-05	Pancreatic Adenocarcinoma
	Badea Pancreas	1.00E-04	Pancreatic Ductal Adenocarcinoma
	Segara Pancreas	1.00E-04	Pancreatic Carcinoma
	Pei Pancreas	1.00E-04	Pancreatic Ductal Adenocarcinoma
GLS1	TCGA	1.00E-04	Pancreatic Adenocarcinoma
	Badea Pancreas	0.05	Pancreatic Ductal Adenocarcinoma
	Segara Pancreas	1.00E-04	Pancreatic Carcinoma
xCT/SLC7A11	Pei Pancreas	9.40E-05	Pancreatic Ductal Adenocarcinoma
	TCGA	0.06 (Grade III Compared to Grade I)	Pancreatic Adenocarcinoma
AKR1C1	Segara Pancreas	1.00E-04	Pancreatic Carcinoma
	TCGA	0.008 (Stage III Compared to Stage I)	Pancreatic Adenocarcinoma
IDH1	Segara Pancreas	1.00E-04	Pancreatic Carcinoma
	Badea Pancreas	1.00E-04	Pancreatic Ductal Adenocarcinoma
	Pei Pancreas	1.00E-04	Pancreatic Ductal Adenocarcinoma
	TCGA	0.02 (Grade III Compared to Grade I)	Pancreatic Adenocarcinoma
GCLM	Segara Pancreas	1.78E-07	Pancreatic Carcinoma
	Badea Pancreas	1.00E-04	Pancreatic Ductal Adenocarcinoma
HMOX1	Badea Pancreas	1.00E-04	Pancreatic Ductal Adenocarcinoma
	TCGA	0.05 (Stage III Compared to Stage I)	Pancreatic Adenocarcinoma
GDH1/GLUD1	Pei Pancreas	0.05	Pancreatic Ductal Adenocarcinoma
	Badea Pancreas	0.05	Pancreatic Ductal Adenocarcinoma
	TCGA	0.01 (Grade III Compared to Grade I)	Pancreatic Adenocarcinoma